Self-Configurable Coordinated Scheduling for Ultra-Dense Small Cell Deployments

Sonia Gimenez, David Martín-Sacristán, Daniel Calabuig, Jose F. Monserrat
iTEAM Research Institute, Universitat Politècnica de València
Camino de Vera S/N, 46022, Valencia, Spain
{sogico, damargan, dacaso, jomondel}@iteam.upv.es

***Abstract*—Mobile networks tend to increase the density of access points, mainly in indoor scenarios where ultra-dense networks of small cells are envisioned for the 5G. The management of this kind of indoor deployments is very challenging and low complexity inter-cell interference coordination techniques are needed to address the situation of massive interference. This paper proposes a self-configurable coordinated scheduling algorithm, based on a distributed fractional frequency reuse scheme. The algorithm is able to adapt to different load conditions, adjusting the frequency reuse pattern and allocating users to the most appropriate frequency band, depending on the distribution of interference. The performance of the algorithm has been assessed through simulations considering cells and users with multiple antennas, configuration in which the interference coordination algorithms do not usually achieve significant gains. Still being feasible and simple to implement, this algorithm achieves a significant improvement in the power consumption and cell-edge user throughput even in low cell density cases. When increasing the number of small cells, results show also an improvement in the average user throughput and cell spectral efficiency.**

***Index Terms*—inter-cell interference coordination, small cells, indoor deployment, fractional frequency reuse.**

I. Introduction

It is forecast that upcoming traffic demands will need a huge increase of network capacity, not only to support the future mobile broadband services but also to allow for a massive connectivity of devices. Since current technologies are not able to satisfy such requirements, research community is working towards the establishment of the fifth generation (5G) of mobile networks. Three main paradigms are being considered as possible enablers to boost network capacity: the increase of the cell spectral efficiency, the use of more spectrum and the ultra-densification of cells [1], [2].

In this framework, Small Cells (SCs) have been shown as a straightforward way to increase network densification for a large variety of target scenarios, including indoor and outdoor deployments, with and without Macrocell (MC) coverage [3]. On the one hand, Heterogenous Networks (HetNets) are defined as scenarios in which nodes with different level of power are deployed in the same coverage area, usually sharing the same frequency band. In particular, outdoor HetNets consist of sets of SCs overlaid on the MCs coverage areas with the aim of off-loading traffic from the MCs to the SCs. However, due to the large difference of transmission power between both types of cells, the area served by an SC may comprise only a few users located in its close proximity, which receive the strongest downlink Received Signal Strength (RSS) from the SC [4]. In order to extend the coverage area of the SCs, the 3rd Generation Partnership Project (3GPP) introduced the use of Cell Range Extension (CRE), based on adding a positive bias to the SCs RSS in the cell selection procedure. Nevertheless, CRE results in an increase of the interference created by the MC to the SC users located at the extended coverage area. In fact, it has been shown that the use of CRE in outdoor HetNets without the application of any Inter-cell Interference Coordination (ICIC) mechanism results in a degradation of the overall network performance due to the inter-tier interference [5].

Considerable efforts have been devoted to design ICIC schemes that solve the inter-tier interference in co-channel SC and MC deployments. With this aim, Almost Blank Subframe (ABS) was introduced by 3GPP as a time-domain enhanced ICIC (eICIC) mechanism [6]. In [7], an extension of the ABS subframe was presented to achieve a fast adaptation of the ABS patterns to the network load conditions and to improve the fairness among users, by means of dynamic muting decisions. A frequency-domain ICIC technique for HetNets with multiple antennas is studied in [8]. This work points out the decrease of the obtained benefit of ICIC application when advanced receivers are implemented, since they are able to suppress inter-cell interference at reception.

Other outdoor deployments where SCs and MCs operate in different frequency bands are studied in [9], [10]. In these networks, there is not inter-tier interference and thus, ICIC schemes focus on the control of the interference generated among the SCs. In [9], the authors proposed a time-domain ICIC algorithm based on ABS. Different ABS ratios and patterns are selected at each SCs, what allows a better adaptation to user distribution and traffic load. Moderate gains are shown only for finite buffer traffic. Additionally, a cognitive ICIC algorithm is presented in [10] for a MC and SC deployment using an architecture which separates control and data planes. An analytical characterization of the received aggregated interference at a user is provided in order to decide whether it will be scheduled at a certain subframe, with the final aim of improving the user throughput. However, this study is limited since the overall network performance was not analysed and only one antenna was considered at both transmission and reception sides.

On the other hand, indoor SC deployments are also usually considered to be isolated from MC interference, due to the penetration losses introduced by the walls of the buildings. The application of ICIC algorithms in such isolated indoor deployments has received less attention by the research community. An adaptive Fractional Frequency Reuse (FFR) scheme for femtocell deployments is presented in [11], showing a large improvement of the cell-edge user throughput but at the expense of a degradation of cell-centre user throughput. Moreover, a self-organized FFR-based allocation algorithm for dense femtocell deployments is proposed in [12], but the obtained results are not compared with the frequency reuse 1 case when no ICIC scheme is applied. Also, a fuzzy logic ICIC scheme is proposed in [13] for a randomly and dense femtocell deployment, showing an improvement of the system performance. Nevertheless, these ICIC solutions for indoor SC deployments consider only single-antenna base stations and users.

Being SCs isolated from the MCs or being them operating in a different band, the studies of ICIC techniques applied to these SC deployments point towards the limited benefit of using FFR schemes [14]. However, further research is required to analyse the suitability of ICIC application on indoor SC deployments with higher density of nodes, which will characterise the incoming 5G system. Furthermore, this paper deals with this topic under the basic assumption of the availability of multiple antennas, which is usually not considered in the literature. For this purpose, a Self-Configurable Coordinated Scheduling (SCCS) algorithm is proposed as a frequency-domain ICIC technique, and the benefit of its application is analyzed with different SC densities.

The remainder of the paper is structured as follows. Section II presents the system model used in this work, while Section III describes the proposed SCCS algorithm. The simulation setup is detailed in Section IV and the main simulation results are collected in Section V. Finally, the key conclusions are summarized in Section VI.

II. System Model

We consider a downlink Orthogonal Frequency Division Multiplexing (OFDM) system with N_{SC} SCs and K User Equipment devices (UEs), working in Frequency Division Duplex (FDD) mode. We denote by N_t and N_r the number of antennas at each SC and UE, respectively. Cell selection is done according to the maximum received power by the user.

Furthermore, in order to exploit the multi-antenna architecture, codebook-based precoding is applied at transmission [15] and a Minimum Mean Square Error (MMSE) receiver is implemented at the UE [16]. The spatial multiplexing of different information streams is not considered in this work.

It is assumed that downlink transmission resources are partitioned in a time-frequency grid. In the time domain, a subframe is defined as the smallest unit of time in which scheduling decisions are made, in a distributed fashion, at the SCs. Channel is considered to remain constant during the subframe period. In the frequency domain, resources are grouped in blocks. The minimum time-frequency resource is known as Resource Block (RB) and consists of one frequency block during one subframe period. The scheduler can allocate a different user per RB. Besides, equal power transmission per RB is considered.

Small cells are connected to the core network using broadband IP, such as DSL or cable modems, and a logical interface is available to support the exchange of control messages among SCs. In order to consider the latencies introduced by the routing and processing of the exchanged messages, certain delay T_D is considered in the messages delivery time.

III. Self-Configurable Coordinated Scheduling for Ultra-Dense Deployments

In this section, we present our proposed Self-Configurable Coordinated Scheduling (SCCS) technique for ultra-dense SC deployments. SCCS is divided into three phases: the clustering, the static configuration, and the dynamic configuration. In the clustering phase, SCs are grouped into non-overlapping clusters, by means of a centralized clustering algorithm. Then, in the static configuration phase, small cells within the same cluster, known as neighbour cells, exchange control messages to decide which resources will be able to use with certain priority at each cell, following a FFR-based pattern. Finally, in the dynamic configuration phase, SCs coordinate their resource scheduling decisions via the exchange of messages, which are able to forbid or allow for the use of specific resources in the neighbours. In an LTE system, all this message exchange can be made with standard X2 messages [17].

A. Clustering phase

In this phase, each user u reports to its serving cell s the interference power received from all the cells in the network, I_j^u, with $j \neq s$. This information is collected by each cell i in the network, which computes the average interference generated by any other cell j on its N_{u_i} users, I_{ij}, according to the following equation:

$$I_{ij} = \frac{1}{N_{u_i}} \sum_{u=1}^{N_{u_i}} I_j^u. \tag{1}$$

A central unit responsible for the clustering procedure collects these values and creates a matrix $\mathbf{I} \in \mathbb{R}^{N_{SC} \times N_{SC}}$, where the $\{i, j\}$ element of the matrix corresponds to the interference value I_{ij}. Using this matrix, the clustering algorithm aims to assign to the same cluster those cells that generate the highest interference to each other, as detailed in Algorithm 1.

B. Static configuration phase

Once the clusters are formed, the frequency reuse pattern to be applied at every cluster is configured. With this aim, total frequency bandwidth W_t available in the system is divided into three different sub-bands: the ordinary sub-band, the preferential sub-band, and the non-preferential sub-band, with W_o, W_p and W_{np} bandwidths, respectively. Fig. 1 shows an example of this per-cluster sub-band configuration, for a cluster composed by 4 small cells.

Algorithm 1 Inputs: set of cells, $\mathcal{S}$; cluster size, C_s; interference matrix $\mathbf{I} \in \mathbb{R}^{|S|\times|S|}$. **Output:** Clusters of cells, $\mathcal{Q}_l, l \leq |\mathcal{S}|$.

$\mathcal{K} := \mathcal{S}$, $\mathcal{Q}_l := \emptyset, \forall l$, $t := 1$
while $|\mathcal{K}| > 0$ **do**
  $\{i^*, j^*\} \leftarrow \arg\max_{(i,j)} \mathbf{I}_{i,j}$
  $\mathcal{Q}_t \leftarrow \mathcal{Q}_t \cup \{i^*, j^*\}$, $\mathcal{K} \leftarrow \mathcal{K} \setminus \{i^*, j^*\}$
  $\mathbf{I}_{s,m} = 0, \mathbf{I}_{m,s} = 0$, for $s \in 1, ..., |\mathcal{S}|$, $m \in \{i^*, j^*\}$
  while $|\mathcal{Q}_t| < C_s$ and $|\mathcal{K}| > 0$ **do**
    $k^* \leftarrow \arg\max_k \mathbf{I}_{s\in\mathcal{Q}_t,k}$
    $\mathcal{Q}_t \leftarrow \mathcal{Q}_t \cup \{k^*\}$, $\mathcal{K} \leftarrow \mathcal{K} \setminus \{k^*\}$
    $\mathbf{I}_{s,k^*} = 0, \mathbf{I}_{k^*,s} = 0$ for $s \in 1, ..., |\mathcal{S}|$
  end
  $t = t + 1$
end

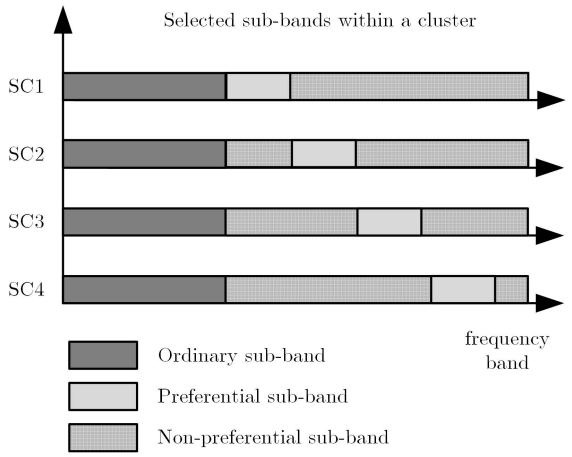

Fig. 1. Example of SCCS per-cluster sub-band configuration, for a cluster composed by 4 small cells.

On the one hand, the ordinary sub-band is common to all the cells in the network and is configured in a statical and centralized fashion, fixing the W_o value. Resources within the ordinary sub-band are always available to be used simultaneously by every cell in the cluster, resulting in a frequency reuse factor of one. Since interference power in the ordinary sub-band is expected to be high, users with good channel conditions are supposed to be allocated in this sub-band.

On the other hand, preferential and non-preferential sub-bands are configured within a cluster by means of the exchange of messages among neighbours. The preferential sub-band at each cell is the set of resources that a cell has the privilege to configure in its neighbours, i.e., to forbid or allow for their use in the neighbour cells. The bandwidth of the preferential sub-band depends on the ordinary bandwidth W_o and the cluster size C_s, and it is computed as:

$$W_p = \lfloor (W_t - W_o)/C_s \rfloor. \quad (2)$$

In case a cell decides to use its preferential sub-band with priority, it will forbid the use of these resources in its neighbours. For that reason, a preferential sub-band in one cell must be non-preferential in the rest of cells within the same cluster, but not the other way around. Therefore, the available resources to be used within the non-preferential sub-band at each cell, defined as $\hat{W}_{np}$, will change over time depending on the scheduling decisions taken at the neighbours. The limits of $\hat{W}_{np}$ are given by:

$$W_t - (W_o + W_p C_s) \leq \hat{W}_{np} \leq W_t - (W_o + W_p), \quad (3)$$

where the lower and upper limits correspond to the cases in which either all or none of the neighbours, respectively, are using their preferential sub-bands with priority.

Cells within a cluster select their preferential sub-bands sequentially, interrogating their neighbours about which set of resources they are using as preferential sub-band. Then, cells select as preferential sub-band one of the sub-bands not already used as preferential in any of the neighbours and out of the ordinary sub-band.

The flexibility of SCCS lies on the ability of cells of using preferential sub-bands with or without priority, depending on which user is allocated to this sub-band. In particular, preferential sub-band is supposed to be used with priority to allocate users with worse channel conditions, also called critical users. In case a cell decides to use its preferential sub-band with priority, it must send a message to the neighbours in order to forbid the use of these resources. Similarly, when a cell decides to use its preferential sub-band without priority, it must send another message to inform the neighbours that those resources are again available to be used.

In practice, a non-preferential RB will be available in a cell only when the neighbours are not using this RB with priority. In order to know the available resources at each subframe, every cell stores a bit-map indicating which RBs have been forbidden or not by the neighbours. Note that when all cells within a cluster are using their corresponding preferential sub-bands without priority, all RBs will be available at every cell and thus, SCCS corresponds to a frequency reuse 1 scheme.

The proper selection of W_o and C_s will determine the correct performance of SCCS, which must be chosen in relation to the SCs and user densities. The optimization of these parameters is beyond the scope of this work.

C. Dynamic configuration phase

In this phase, user scheduling is performed taking into account the available resources at each cell, determined by the stored bit-maps. Moreover, each cell decides autonomously on the usage with or without priority of its preferential sub-band, depending on whether any of its users has been classified as critical or not.

User classification is performed periodically, with a configurable period T_u equal for all users. However, users are not classified simultaneously. Classification of each user k is done by its serving cell s according to the following procedure. It is assumed that the rest of users at cell s have been already classified, resulting in N_c critical and N_{nc} non-critical users. Furthermore, the estimated Signal to Noise plus Interference ratio (SINR) experienced by user k when classified as critical is defined as SINR_c^k, while SINR_{nc}^k represents the estimated SINR when it is classified as non-critical. SINR estimation is

computed taking into account the long term average interference experienced by each user at the corresponding sub-band. Therefore, the expected throughput achieved by user k if it is classified as critical, Th_c^k, is given by

$$Th_c^k = \frac{W_p}{N_c + 1} \min(\beta, \log_2(1 + \text{SINR}_c^k)), \quad (4)$$

while the throughput achieved by user k when it is classified as non-critical, is given by

$$Th_{nc}^k = \frac{\hat{W}_{np} + W_o}{N_{nc} + 1} \min(\beta, \log_2(1 + \text{SINR}_{nc}^k)), \quad (5)$$

where the min operation models the upper bound of the efficiency, represented by β, due to the limitation of the available modulation schemes. Finally, cell s classifies user k as critical when $Th_c^k > Th_{nc}^k$, and as non-critical otherwise. Note that some changes in the user classification imply the exchange of control messages. Specifically, a change of N_c from 1 to 0 will force sending a message to the neighbours with the aim of releasing some RBs. Contrarily, changing N_c from 0 to 1 will result in a message to forbid temporarily the use of the same resources.

After the classification, critical users will be allocated to preferential sub-bands while ordinary sub-band and available RBs within non-preferential sub-band will be used to allocate non-critical users.

IV. Simulation Setup

A. Channel modelling

We consider the Indoor Hotspot (InH) channel model proposed by the Radiocommunication Sector of the International Telecommunication Union (ITU-R) in [18]. Simulations are conducted using a carrier frequency of 3.4 GHz and a system bandwidth of 20 MHz. Perfect channel estimation is assumed at the transmitter and receiver side, although channel estimation period is considered greater than the subframe duration.

B. Deployment considerations

Simulation setup consists of a rectangular floor spanning 120 m $\times$ 50 m. The number of deployed SCs varies from 2 to 18, being the exact locations of cells collected in Table I. User density has been set to 3 users per 100 m^2, resulting in a total number of 180 users randomly distributed in the area. Other important simulation parameters are listed in Table II.

Regarding the SCCS algorithm, first classification instant of each user in the system, t_c, is modelled as a uniformly-distributed random variable in the interval $[0, T_m]$, in order to avoid the simultaneous classification of all the users and guarantee classification convergence. Table III collects the main parameters used for the configuration of SCCS. W_o and C_s have been chosen to optimize the performance of SCCS in this scenario, after an exhaustive search considering a limited set of values.

TABLE I
SMALL CELLS LOCATION OF ALL SIMULATED DEPLOYMENTS.

	X [m]	Y [m]
2 SCs	30,90	25
4 SCs	15,45,75,105	25
8 SCs	15,45,75,105	15,35
12 SCs	10,30,50,70,90,110	15,35
18 SCs	10,30,50,70,90,110	12.5,25,37

TABLE II
SIMULATION PARAMETERS.

Number of simulated drops	30
Simulation time per drop	1 s
Subframe duration	1 ms
Channel estimation period	6 ms
Number of RBs	100
RB bandwith	180 kHz
Scheduling policy	Round Robin
Thermal noise PSD	-174 dBm/Hz
Cell Tx Power, P_t	21 dBm
UE noise figure	5 dB
UE speed	3 km/h
BS height	6 m
UE height	1.5 m
Min UE-BS distance	3 m
Number of antennas at the SC, N_t	2
Number of antennas at the UE, N_r	2
Upper bound of efficiency, β	6 b/s/Hz

TABLE III
SCCS CONFIGURATION PARAMETERS.

Ordinary sub-band bandwidth, W_o	$0.6 \times W_t$
Maximum cluster size, C_s	2
Message delivery delay, T_D	5 ms
User classification update period, T_u	10 ms
Max initial clas. instant, T_m	50 ms

V. Simulation Results

In this section, the numerical results obtained through system level simulations for the different deployments detailed in Section IV are presented. We compare the performance of the proposed SCCS algorithm to the baseline, in which no ICIC technique is applied.

The Cumulative Distribution Function (CDF) of the linear average SINR at the receiver is shown in Fig. 2, for the case of 2, 8 and 18 deployed SCs. As expected, CDF curves show for both algorithms a reduction of the SINR values as the density of SCs increases, due to the lower inter-cell distance and the consequent higher interference in the system. Besides, the application of SCCS achieves an improvement in the SINR with respect to the baseline, thanks to its ability to suppress, over certain sub-bands, the interference caused by the cells to their neighbours. Nevertheless, the gain in SINR obtained by SCCS becomes smaller as long as the number of SCs increases, caused by the fixed value of the cluster size C_s used in the simulations, which limits the number of increasing interferers the algorithm is able to combat.

Furthermore, the CDF of the user throughput is represented in Fig. 3. These curves show how an increase on the SINR val-

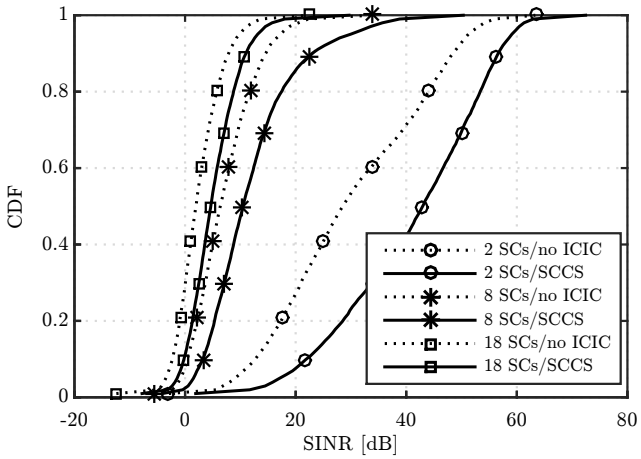

Fig. 2. CDF of the user SINR.

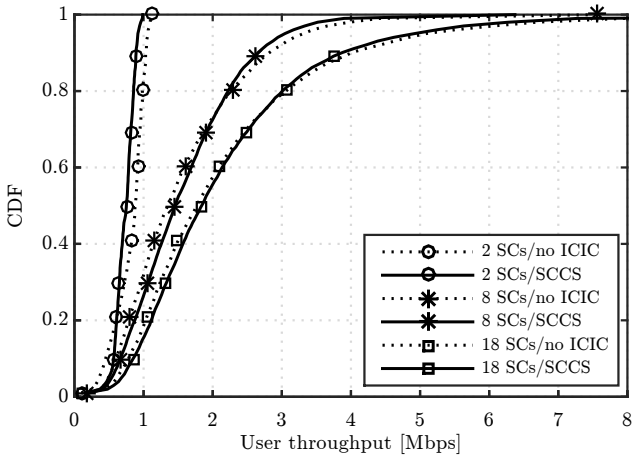

Fig. 3. CDF of the user throughput.

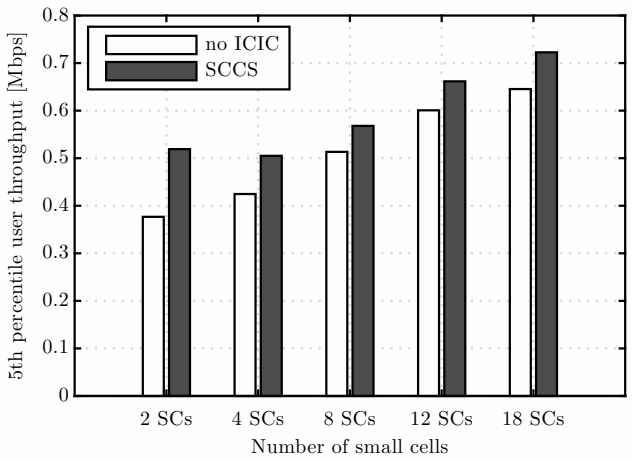

Fig. 4. 5th percentile of user throughput.

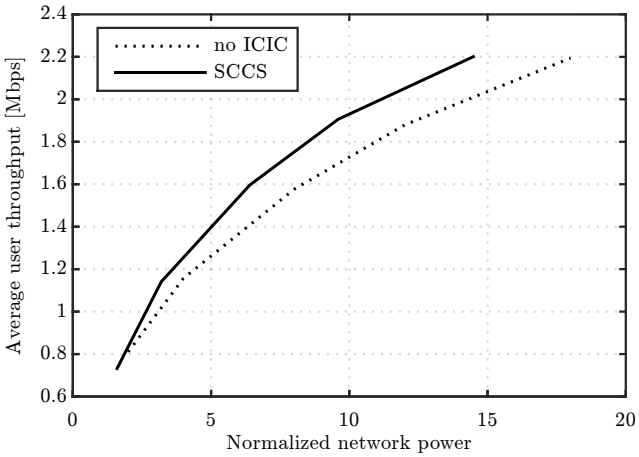

Fig. 5. Average user throughput versus normalized network power.

ues not always results in higher user throughput values, since the application of SCCS implies a reduction in the number of available resources per cell. Indeed, a better performance of SCCS with respect to the baseline is observed mainly for the lower throughput values of the CDF, resulting in an increase of the fairness among users. These lower throughput values correspond to users experiencing bad channel conditions, which obtain a benefit for being allocated to the preferential sub-bands thanks to the lower level of interference existing on them, even when $W_p \ll (W_o + \hat{W}_{np})$. Contrarily, users with better channel conditions, allocated mainly to the ordinary and non-preferential sub-bands, worsen their achieved throughput values since bandwidth available for transmission, $W_o + \hat{W}_{np}$, is smaller than the total bandwidth W_t available when no ICIC is applied.

The 5th percentile of the user throughput is depicted in Fig. 4 for both algorithms, as a function of the number of deployed small cells. It is shown how the application of SCCS algorithm provides a significant increase of the 5th percentile user throughput with respect to the baseline, for every density of deployed small cells. Note that the higher 5th percentile user throughput benefit obtained for the deployment with 2 SCs can be justified considering that interference is completely removed for the users allocated to the preferential sub-band of each cell, since not interference sources exist out of the cluster. For the rest of cell densities, above a 10% of gain in the 5th percentile user throughput is achieved for all cases.

On the other hand, average user throughput and cell spectral efficiency values are collected in Table IV, for all the simulated deployments. Also, the gain achieved by SCCS with respect to the baseline is presented for these performance indicators. If we focus on the absolute values of the average user throughput, it is shown how increasing the number of cells improves the average user throughput in the network. However, the increase of interference brought by the higher density of cells results in a decrease of the cell spectral efficiency. Regarding the comparison of SCCS with the baseline, it is observed that for deployments with less than 4 SCs the gain showed in 5th user throughput comes at expenses of a decrease of the average user throughput. Contrarily, for deployments with more than 4 SCs the application of the ICIC algorithm achieves gains in 5th user throughput while maintaining the average user

TABLE IV
AVERAGE USER THROUGHPUT AND CELL SPECTRAL EFFICIENCY.

	2 SCs		4 SCs		8 SCs		12 SCs		18 SCs	
	no ICIC	**SCCS**	**no ICIC**	**SCCS**	**no ICIC**	**SCCS**	**no ICIC**	**SCCS**	**no ICIC**	**SCCS**
Average user throughput [Mbps]	0.81	0.73	1.16	1.14	1.58	1.60	1.88	1.91	2.19	2.20
Gain	-	-9.6%	-	-1.4%	-	+1.3%	-	+1.4%	-	+0.3%
Cell spectral efficiency [Mbps/Hz]	3.65	3.30	2.60	2.57	1.77	1.80	1.41	1.43	1.10	1.10
Gain	-	-9.5%	-	-1.2%	-	+1.4%	-	+1.7%	-	+0.4%

throughput. This result reveals that high density deployments with multiple antennas can take profit of the application of ICIC schemes from a cell spectral efficiency point of view.

Finally, it is worth highlighting the power saving achieved thanks to the application of SCCS. For this purpose, Fig. 5 represents the average user throughput as a function of the total power used by the network normalized with respect to the SC transmission power P_t. It is easily observable that a lower amount of power is required by SCCS algorithm to achieve a certain average user throughput value. In fact, the difference of required power between both algorithms becomes greater as the target average user throughput is higher. Also, another important conclusion drawn from this result is that SCCS allows achieving higher average user throughput by means of densification still using the same amount of total power in the network.

VI. CONCLUSION

In this work, an assessment of the suitability of ICIC application on ultra-dense indoor small cell deployments has been performed. For this purpose, a self-configurable coordinated scheduling algorithm has been proposed as a frequency-domain ICIC technique, based on a FFR scheme. System level simulations have been carried out considering a downlink indoor deployment with multiple antennas and different densities of deployed small cells. Simulation results have shown that SCCS improves the 5th percentile user throughput independently on the number of deployed small cells. For high density deployments, also an increase of the average user throughput is achieved, resulting in larger cell spectral efficiency values. Furthermore, the proposed SCCS algorithm has shown an important reduction of the SC power consumption, which results in more power efficient deployments.

As future work, it is of interest to study the performance of the proposed algorithm when small cells are configured in closed subscriber group mode. Moreover, the optimization of the sub-bands configuration with respect to the user distribution is also a future line of research.

ACKNOWLEDGEMENT

This work has been supported by the Ministerio de Economia y Competitividad, Spain (TEC2011-27723-C02-02 and TEC2014-60258-C2-1-R), by the European FEDER funds.

REFERENCES

[1] V. Jungnickel, K. Manolakis, W. Zirwas, B. Panzner, V. Braun, M. Lossow, M. Sternad, R. Apelfrojd, and T. Svensson, "The role of small cells, coordinated multipoint, and massive MIMO in 5G," *IEEE Communications Magazine*, vol. 52, no. 5, May 2014.

[2] J. F. Monserrat, H. Droste, O. Bulakci, J. Eichinger, O. Queseth, M. Stamatelatos, H. Tullberg, V. Venkatkumar, G. Zimmermann, U. Dotsch, and A. Osseiran, "Rethinking the mobile and wireless network architecture: The METIS research into 5G," in *European Conference on Networks and Communications (EuCNC)*, June 2014.

[3] 3GPP TSG RAN, "Scenarios and requirements for small cell enhancements for E-UTRA and E-UTRAN (Release 12)," TR 36.932 (V12.1.0), Tech. Rep., March 2013.

[4] D. López-Pérez, I. Guvenc, G. de la Roche, M. Kountouris, T. Q. S. Quek, and J. Zhang, "Enhanced intercell interference coordination challenges in heterogeneous networks," *IEEE Wireless Communications*, vol. 18, no. 3, June 2011.

[5] D. López-Pérez, M. Ding, H. Claussen, and A. H. Jafari, "Towards 1 Gbps/UE in cellular systems: Understanding ultra-dense small cell deployments," *IEEE Communications Surveys Tutorials*, vol. 17, no. 4, June 2015.

[6] H. Holma, A. Toskala, and J. Reunanen, *LTE Small Cell Optimization: 3GPP Evolution to Release 13*. Wiley, January 2016.

[7] B. Soret and K. I. Pedersen, "Centralized and distributed solutions for fast muting adaptation in LTE-Advanced HetNets," *IEEE Transactions on Vehicular Technology*, vol. 64, January 2015.

[8] P. Luoto, J. Leinonen, P. Pirinen, V. V. Phan, and M. Latva-aho, "Bitmap based resource partitioning in LTE-A femto deployment," in *IEEE International Conference on Communications (ICC), 2013*, June 2013.

[9] J. Wang, L. Liu, K. Takeda, and H. Jiang, "Time domain inter-cell interference coordination for dense small cell deployments," in *IEEE 80th Vehicular Technology Conference (VTC Fall)*, September 2014.

[10] S. A. R. Zaidi, D. C. McLernon, M. Ghogho, and M. A. Imran, "Cloud empowered cognitive inter-cell interference coordination for small cellular networks," in *IEEE International Conference on Communication Workshop (ICCW)*, June 2015.

[11] G. Huang and J. Li, "Interference mitigation for femtocell networks via adaptive frequency reuse," *IEEE Transactions on Vehicular Technology*, 2015.

[12] Y. Wu, H. Jiang, and D. Zhang, "A novel coordinated spectrum assignment scheme for densely deployed enterprise LTE femtocells," in *IEEE 75th Vehicular Technology Conference (VTC Spring)*, May 2012.

[13] H. Burchardt, S. Sinanovic, Z. Bharucha, and H. Haas, "Distributed and autonomous resource and power allocation for wireless networks," *IEEE Transactions on Communications*, vol. 61, July 2013.

[14] R. Ghaffar and R. Knopp, "Fractional frequency reuse and interference suppression for OFDMA networks," in *8th International Symposium on Modeling and Optimization in Mobile, Ad Hoc, and Wireless Networks*, May 2010.

[15] J. Wang, M. Wu, and F. Zheng, "The codebook design for MIMO precoding systems in LTE and LTE-A," in *6th International Conference on Wireless Communications Networking and Mobile Computing (WiCOM), 2010*, September 2010.

[16] H. Busche, A. Vanaev, and H. Rohling, "SVD-based MIMO precoding and equalization schemes for realistic channel knowledge: Design criteria and performance evaluation," *Wireless Personal Communications*, vol. 48, February 2009.

[17] S. Gimenez, D. Calabuig, J. F. Monserrat, and N. Cardona, "Dynamic and load-adapting distributed fractional frequency reuse algorithm for ultra-dense networks," *Waves*, vol. 7, June 2015.

[18] ITU-R, "Guidelines for evaluation of radio interface technologies for IMT-Advanced," Tech. Rep. M.2135-1, 2009.